Reactions of Laser-Ablated Niobium and Tantalum Atoms with Oxygen Molecules: Infrared Spectra of Niobium and Tantalum Oxide Molecules, Anions, and Cations

Mingfei Zhou and Lester Andrews*

University of Virginia, Department of Chemistry, Charlottesville, Virginia 22901

Received: May 12, 1998; In Final Form: July 28, 1998

Laser-ablated niobium and tantalum atoms react with O_2 to give MO, MO_2, MO_2^-, and MO_2^+ products, which are identified from oxygen isotopic substitution on their matrix infrared spectra and from DFT calculations of isotopic frequencies. Annealing allows diffusion and further reaction to form $(O_2)MO_2$ complexes, which are characterized by four fundamentals. On the basis of the ν_3 vibrational frequencies for the $M^{16}O_2$ and $M^{18}O_2$ isotopic molecules, the metal dioxide valence angles are estimated to be 108 ± 5° for NbO_2 and 106 ± 5° for TaO_2; the molecular cations have the smaller valence angles 103 ± 5° and 105 ± 5° for NbO_2^+ and TaO_2^+, respectively, and the molecular anions are more open with 120 ± 10° valence angles. Evidence is also presented for stable MO_3^- anion species.

Introduction

In the past several decades, numerious studies have been conducted on niobium and tantalum oxides due to their importance in high-temperature chemistry and stellar atmospheres.[1] Diatomic niobium and tantalum oxides have been extensively studied spectroscopically in the gas phase as well as in solid matrixes.[2−12] The electronic ground state of NbO was determined to be $^4\Sigma^-$ from ESR and optical spectroscopic studies in inert matrices,[9] whereas the ground state of TaO was derived as $^2\Delta$ from optical spectra in the matrix[6] as well as the gas phase.[7] Infrared vibrational fundamentals of the NbO, TaO, and TaO_2 molecules have been reported,[6,8] and the dissociation and ionization energies have been determined for NbO and TaO by mass spectrometric and photoelectron spectroscopic experiments.[13−15] Hartree−Fock−Slater calculations on diatomic oxides and cations have been performed.[15] Thermal bimolecular reactions of niobium cluster ions with oxygen have been reported,[15−17] and the reactivities of metal oxide cluster ions have also been studied in the gas phase;[18] however, little is known about reactions of the metal atoms with oxygen molecules.

Recent investigations of laser-ablated transition metal atoms with oxygen[19−26] have shown very rich chemistry due to high reactivity of the ablated metal atoms, and more products were observed as compared to ordinary thermal atom reactions. The vanadium−oxygen system contained a large number of product molecules: VO, VO_2 and their dimers, VO_2^-, and a VO_2 complex with O_2 were characterized.[24] In particular, the observation of O_4^+ and O_4^- cluster ions in these experiments underscores the possibility of trapping charged metal oxide species, and evidence for several MO_2^- anions has been presented. This paper reports similar studies of laser-ablated niobium and tantalum atom reactions with oxygen molecules during condensation in excess argon.

Experimental Section

The technique for laser ablation and FTIR matrix investigation has been described previously.[27,28] Niobium and tantalum metal targets (Goodfellow, 99%; Mackay, 99.99%) were mounted on a rotating rod. The Nd:YAG laser fundamental (1064 nm, 10 Hz repetition rate, 10 ns pulse width) was focused on the rotating target through a hole in the CsI cryogenic (10 K) window using 40−80 mJ/pulses. The ablated metal atoms were co-deposited with 0.25−1.0% O_2 in argon at 2−4 mmol/h for 1−2 h. Isotopic $^{18}O_2$ as well as mixed $^{16}O_2 + {}^{18}O_2$ and scrambled $^{16}O_2 + {}^{16}O^{18}O + {}^{18}O_2$ samples were used for band identification.

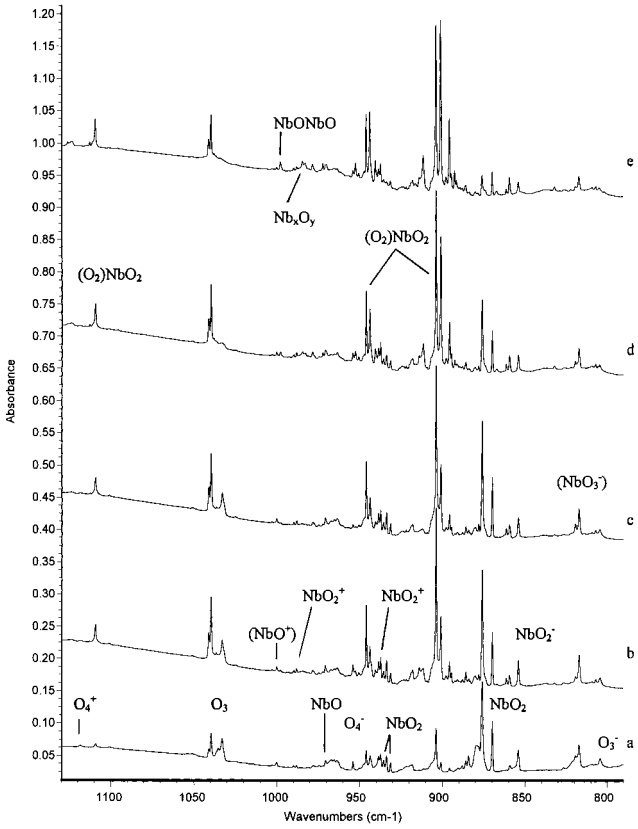

Figure 1. Infrared spectra of products formed by reactions of laser-ablated Nb atoms with O_2 (0.5%) in argon on condensation at 10 K: (a) co-deposited sample, (b) after 25 K annealing, (c) after broad-band photolysis for 20 m, (d) after 30 K anealing, and (e) after 35 K annealing.

10.1021/jp982212c CCC: $15.00
Published on Web 10/06/1998

TABLE 1: Infrared Absorptions (cm^{-1}) from Co-Deposition of Laser-Ablated Niobium Atoms with Oxygen in Excess Argon at 10 K

$^{16}O_2$	$^{18}O_2$	$^{16}O_2 + {}^{16}O^{18}O + {}^{18}O_2$	R(16/18)	ann/phot[a]	assignment
1118.7	1056.0		1.0594	− −/−	O_4^+
1126.2	1062.5	1096.1	1.0599	++/	$(O_2)_xNbO_2$
1123.1	1059.5	1092.8	1.0600		$(O_2)_xNbO_2$
1112.6	1049.9		1.0597	++/o	$(O_2)_xNbO_2$
1109.3	1046.6	1109.3, 1078.4, 1046.6	1.0599	+ −/o	$(O_2)NbO_2$
1039.5	982.3		1.0582	+ −/−	O_3
1033.0	976.2		1.0582	+ −/−	O_3, site
1000.1	951.5		1.0510	− −/o	(NbO^+)
997.6	949.7	997.6, 978.1, 964.3, 949.7	1.0504	+ +/o	NbONbO
989.7	940.6		1.0522	+ −/o	NbO_2^+, ν_1
988.0	939.1		1.0521	+ −/o	NbO_2^+, ν_1
982.7	936.5		1.0493	+ +/o	Nb_xO_y
970.6	923.5	970.6, 923.5	1.0510	+ −/o	NbO
967.4	920.2	967.4, 920.2	1.0513	− −/o	NbO site
965.2	918.1	965.2, 918.1	1.0513	− −/o	NbO site
963.7	916.6	963.7, 916.6	1.0513	− −/o	NbO site
953.8	901.6		1.0579	− −/−	O_4^-
952.3	904.2		1.0532	+ +/o	$(O_2)NbO_2$, ν_1
945.9	898.3	945.9, 931.9, 898.3	1.0530	+ −/o	$(O_2)NbO_2$, ν_1
943.5	896.1	943.5, 929.6, 896.1	1.0529	+ +/o	(O_2) NbO_2, ν_1, site
940.2	893.2		1.0526	+ +/o	$(O_2)_xNbO_2$
938.4	894.6		1.0490	+ −/o	NbO_2^+, ν_3
937.1	893.4	937.1, 906.0, 893.4	1.0489	+ -/o	NbO_2^+, ν_3
933.5	886.9	933.4, 917.7, 886.9	1.0525	+ −/o	ONbO,ν_1,
931.1	884.4		1.0528	+ −/o	ONbO,ν_1, site
911.3	869.5	911.3, 880.3, 869.5	1.0481	+ +/o	$(O_2)NbO_2$ site
903.6	862.6	903.6, 873.2, 862.6	1.0475	+ −/o	$(O_2)NbO_2$
900.7	859.8	900.7, 870.5, 859.8	1.0476	+ +/o	$(O_2)NbO_2$
895.5	854.9	895.5, 865.8, 854.9	1.0475	+ +/o	$(O_2)_xNbO_2$
892.3	852.1		1.0472	+ +/o	$(O_2)_xNbO_2$
875.9	835.5	875.8, 848.1, 835.6	1.0484	+ −/o	ONbO,ν_3
869.8	829.9	869.8, 842.8, 829.9	1.0481	+ −/o	ONbO,ν_3,site
861.3	822.3		1.0474	+ −/o	$(N_2)NbO_2$
859.4	820.9		1.0469	+ −/o	$(N_2)NbO_2$ site
854.1	816.3	854.1, 824.5, 816.3	1.0463	+ −/−	NbO_2^-
817.1	781.4	816.7, 794.3, 787.1,781.5	1.0457	+ −/−	NbO_3^-
804.4	759.0		1.0598	− −/−	O_3^-
687.6	655.5	687.7, 655.6	1.0490	+ −/−	?
559.3	534.0	558.5, 547.0, 534.4	1.0474	− −/o	Nb_xO_y
511.3	487.4	510.3, 488.1	1.0490	+ −/o	$(O_2)NbO_2$
461.9	438.6		1.0531	+ −/o	Nb_xO_y

[a] Annealing behavior: on first annealing to 25 K and on subsequent annealing to 30−40 K, + notes increase, − notes decrease/broad-band photolysis behavior: + denotes increase, o denotes no change, − denotes decrease.

FTIR spectra were recorded on a Nicolet 750 with 0.5 cm^{-1} resolution and 0.1 cm^{-1} accuracy. Matrix samples were temperature cycled, and selected samples were subjected to broad-band (240−580 nm) photolysis by a medium-pressure mercury arc lamp (Philips, 175 W) with globe removed.

Results

Matrix infrared spectra and DFT calculations of laser-ablated Nb and Ta reaction products with oxygen will be presented.

Nb + O_2/Ar. The infrared spectra of laser-ablated niobium atoms co-deposited with O_2 in excess argon are shown in Figure 1, and absorptions are listed in Table 1. Sharp strong bands at 875.9 and 869.8 cm^{-1} along with the weak bands at 933.5 and 931.1 cm^{-1} and weak doublets at 938.4 and 937.1 and at 989.7 and 988.0 cm^{-1} were observed after deposition. These bands slightly increased on annealing to 25 K and then decreased on higher temperature annealings. A sharp weak band at 1000.1 cm^{-1} and a band with sharp features at 970.6, 967.4, 965.2, and 963.7 cm^{-1} appeared on deposition and decreased on annealing. Strong bands at 945.7 and 903.6 cm^{-1} and very weak bands at 1109.3 and 511.3 cm^{-1} absorption markedly increased on 25 K annealing (Figure 1b). Broad-band photolysis was done after 25 K annealing, and the photolysis behavior is summarized in Table 1; most notable is the decrease in bands at 953.8, 854.1, and 817.1 cm^{-1} (Figure 1c). The 945.7 and 903.6 cm^{-1} bands decreased on subsequent higher temperature annealing while associated 943.5 and 900.7 cm^{-1} bands greatly increased (Figure 1d,e). Sharp 854.1, 817.1, and 559.3 cm^{-1} bands were also produced on deposition, slightly increased on 25 K annealing, and then decreased on higher temperature annealings. The latter also produced sharp bands at 997.6, 952.3, 940.2, 911.3, 895.5, 892.4, and 687.6 cm^{-1}. In addition, O_3 absorptions at 1039.5 and 1033.0 cm^{-1} and weak O_4^+, O_4^-, and O_3^- absorptions at 1118.7, 953.8, and 804.5 cm^{-1}, respectively, were observed after deposition and decreased on annealing and photolysis.[29,30]

Experiments with different laser powers and oxygen concentrations were done; all the product absorptions increased with higher laser power, while in general the relative intensities of product absorptions did not depend significantly on laser power and oxygen concentration.

Oxygen isotopic substitution was employed for band identification, and the $^{18}O_2$ band positions are listed in Table 1. Mixtures ($^{16}O_2$ + $^{18}O_2$ and $^{16}O_2$ + $^{16}O^{18}O$ + $^{18}O_2$) were also investigated. In the experiment with scrambled isotopic oxygen, triplets were observed for absorptions at 1109.3, 945.7, 943.5, 940.2, 938.4, 937.1, 903.6, 900.7, 895.5, 875.9, 869.8, 854.1,

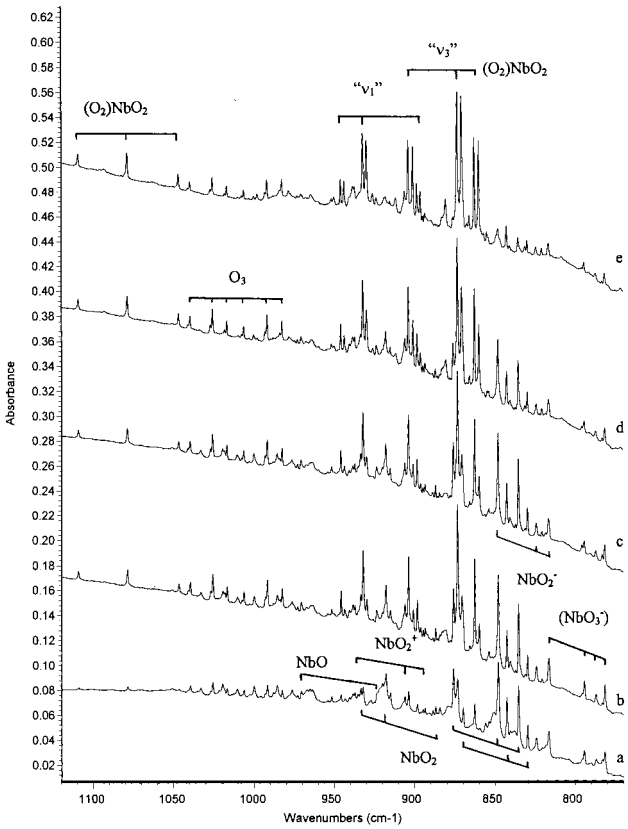

Figure 2. Infrared spectra of products formed by reactions of laser-ablated Nb with oxygen (0.5% in argon, scrambled $^{16}O_2 + {}^{16}O^{18}O + {}^{18}O_2$ mixture, approximately 1:2:1): (a) co-deposited sample, (b) after 25 K annealing, (c) after broad-band photolysis for 20 m, (d) after 30 K anealing, and (e) after 35 K annealing.

and 687.6 cm^{-1}; a quartet was produced for the 817.1 cm^{-1} band, and a broad doublet was observed for the 511.3 cm^{-1} feature. Spectra from the scrambled isotopic sample are shown in Figure 2.

Ta + O_2/Ar. The Ta + O_2 reaction was very similar to the Nb + O_2 system. The spectra are shown in Figure 3 and absorptions are listed in Table 2. Deposition produced strong bands at 906.9 and 904.1 cm^{-1} and weak corresponding bands at 965.3 and 963.0 cm^{-1}. Sharp bands at 1018.1,1014.2, and 1011.7 cm^{-1} also appeared on deposition. All these bands decreased on annealing. Sharp, weak doublets were observed at 993.1 and 991.5 cm^{-1} and at 938.7, 937.3 cm^{-1} after deposition decreased together on annealing. Sharp bands at 952.0 and 896.0 cm^{-1} and at 950.5 and 894.5 cm^{-1} were weak after deposition, but annealing to 25 K markedly increased the 950.5 and 894.5 cm^{-1} bands and destroyed the 952.0 and 896.0 cm^{-1} bands (Figure 3b). Photolysis reproduced the 952.0 and 896.0 cm^{-1} bands and decreased the 950.5 and 894.5 cm^{-1} absorptions about 40% (Figure 3c); annealing and photolysis behavior are summarized in Table 2. The 950.5 and 894.5 cm^{-1} bands were the dominant features in the spectrum after annealing. Two pairs of sharp bands at 946.3 and 889.4 cm^{-1} and at 944.0 and 886.2 cm^{-1} appeared and increased on subsequent annealing. Weak absorptions at 1095.7 and 524.2 cm^{-1} were present on 25 K annealing and tracked on further annealing and photolysis in all experiments. Sharp bands at 836.9, 807.0, and 536.9 cm^{-1} appeared on deposition, increased on annealing to 25 K, and decreased on higher temperature annealings, which produced extra bands at 689.1, 622.4, and 621.0 cm^{-1}.

Again, isotopic substitution experiments were done, and $^{18}O_2$ band positions are given in Table 2. The bands at 1095.7, 952.0, 950.5, 946.3, 944.0, 938.7, 937.3, 912.0, 906.9, 904.1, 896.0, 894.5, 889.4, and 886.2 cm^{-1} produced doublets in $^{16}O_2 + {}^{18}O_2$ isotopic mixture and triplets in $^{16}O_2 + {}^{16}O^{18}O + {}^{18}O_2$ scrambled isotopic experiments. Triplets for 836.9 and 689.1 cm^{-1} and a quartet for 807.0 cm^{-1} bands were observed in both mixed isotopic experiments. Figure 4 illustrates the scrambled isotopic spectrum.

Calculations. DFT calculations were done for NbO, TaO, NbO_2, and TaO_2 molecules using the Gaussian 94 program.[31] The BP86 functional and D95* basis sets on O atom and Los

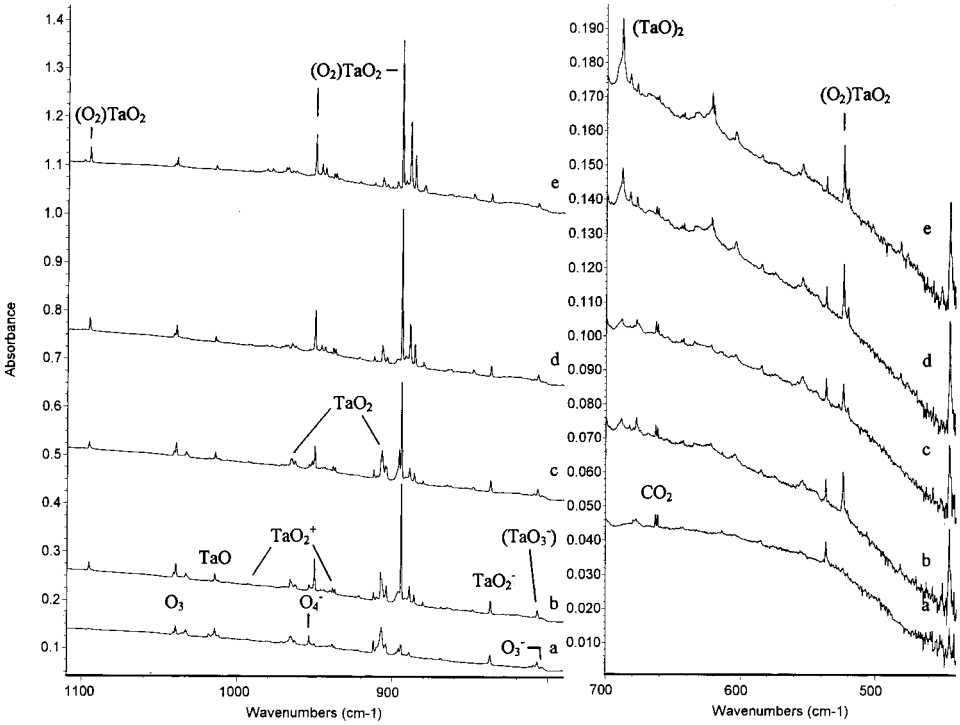

Figure 3. Infrared spectra of products formed by reactions of laser-ablated Ta atoms with O_2 (0.5%) in argon on condensation at 10 K: (a) co-deposited sample, (b) after 25 K annealing, (c) after broad-band photolysis for 20 m, (d) after 30 K anealing, and (e) after 35K annealing.

TABLE 2: Infrared Absorptions (cm^{-1}) from Co-Deposition of Laser-Ablated Tantalum Atoms with Oxygen in Excess Argon at 10 K

$^{16}O_2$	$^{18}O_2$	$^{16}O_2 + {}^{16}O^{18}O + {}^{18}O_2$	R(16/18)	ann/phot[a]	assignment
1124.2	1060.9		1.0597	+ +/o	$(O_2)_xTaO_2$
1118.7	1056.0		1.0594	− −/−	O_4^+
1099.5	1037.6		1.0597	+ +/o	$(O_2)TaO_2$ site
1095.7	1033.9	1095.7, 1065.3, 1033.9	1.0598	+ +/o	$(O_2)TaO_2$
1039.5	982.3		1.0582	+ −/−	O_3
1033.0	976.2		1.0582	+ −/−	O_3
1018.1	964.9	1018.1, 964.9	1.0551	+ −/o	(TaO^+)
1014.2	961.3	1014.2, 961.3	1.0550	− −/o	TaO
1011.7	959.0	1011.7, 959.0	1.0550	− −/o	TaO, site
993.1	940.5		1.0559	− −/o	TaO_2^+, ν_1
991.5	939.0		1.0559	− −/o	TaO_2^+, ν_1 site
978.3	927.3		1.0550	− −/o	Ta_xO_y
971.0	921.0		1.0543	++	Ta_xO_y
968.0	917.4		1.0552	+ +	Ta_xO_y
965.3	914.3	964.9, 949.3, 914.3	1.0558	o −/o	OTaO, ν_1
963.0	912.0		1.0559	+ −/o	OTaO, ν_1 site
953.8	901.8		1.0577	− −/−	O_4^-
952.0	901.1		1.0565	− −/+	$(O_2)TaO_2$ site
950.5	899.4	950.5, 934.0, 899.4	1.0568	++/−	$(O_2)TaO_2$,ν_1
946.3	895.6		1.0566	+ +/o	$(O_2)TaO_2$ site
944.0	893.4		1.0566	+ +	$(O_2)_xTaO_2$
938.8	890.9	938.8, 904.4, 890.9	1.0538	+ −/o	TaO_2^+, ν_3
937.4	889.5	937.2, 903.3, 889.5	1.0539	+ −/o	TaO_2^+, ν_3
933.6	884.0		1.0561	+ +	Ta_xO_y
912.2	865.6	912.2, 879.8, 865.6	1.0538	− −/o	OTaO, ν_3
906.9	860.7	906.9, 875.1, 860.7	1.0537	− −/o	OTaO, ν_3
904.1	858.0		1.0537	+ −/o	OTaO, ν_3 site
896.0	850.8	896.0, 865.4, 850.8	1.0531	− −/+	$(O)_2TaO_2$ site
894.5	849.4	894.5, 862.7, 849.4	1.0531	+ +/−	$(O_2)TaO_2$, ν_3
889.4	844.4	889.4, 857.8, 844.4	1.0533	+ +/o	$(O_2)_xTaO_2$ site
886.2	841.5	886.2, 855.1, 841.5	1.0531	+ +/o	$(O_2)_xTaO_2$
879.9	835.8		1.0528	+ +/o	Ta_xO_y
848.3	805.7	819.0, 805.8	1.0529	+ +/o	Ta_xO_y
836.9	795.3	836.9, 807.6, 795.3	1.0523	+ −/−	TaO_2^-
807.0	766.9	807.6, 786.8, 775.8, 767.0	1.0523	+ −/−	TaO_3^-
804.4	759.0		1.0598	− −/−	O_3^-
689.1	653.4	688.6, 672.2, 653.7	1.0546	++/−	$(TaO)_2$
622.4	590.2	622.2, 602.9, 590.3	1.0546	+ +/o	Ta_xO_y
536.9	510.7	536.7, 524.4, 510.8	1.0513	− −/o	Ta_xO_y
524.2	496.9	524.3, 522.4, 499.1, 496.9,	1.0549	+ +/o	$(O_2)TaO_2$
445.0	423.3	445, 423	1.0513	+ +/o	Ta_xO_y

[a] Annealing behavior: on first annealing to 25 K and on subsequent annealing to 30−40 K, + notes increase, − notes decrease/broad-band photolysis behavior: + denotes increase, o denotes no change, − denotes decrease.

Alamos ECP plus DZ on metal atoms were used. The ground state of NbO was calculated to be a quartet with 1.71 Å bond length and 993.5 cm^{-1} vibrational fundamental. Unlike the other two metal diatomic oxides in this group, TaO was calculated to have a doublet ground state, which is in accord with the experimental observations.[6,7] Both NbO_2 and TaO_2 were calculated to have $^2A_1$ ground states at this level of theory. The $M(O_2)$ and MOO isomers were determined to be much higher in energy and are not listed here. The large energy gap between the bent dioxide and cyclic and asymmetric isomers is in agreement with the absence of $M(O_2)$ and MOO molecules in the spectra; these molecules were major products in the Fe + O_2 and Ni + O_2 reactions.[20,22]

Similar calculations were also done for anions and cations as listed in Table 3. The singlet dioxide anions were more stable, but the triplet states are close enough not to be ruled out. The dioxide cations are predicted to have $^1A_1$ ground states. Both NbO^+ and TaO^+ were calculated to be triplet ground states, the ionization energies calculated here as 7.5 and 8.8 eV were very close to the experimental values: 7.9 and 8.6 eV.[15] Calculations were also done for trioxide molecules and anions, and the latter were found to be very stable with very strong antisymmetric stretching modes, as listed in Table 4.

DFT calculations were done for $OONbO_2$ and $(O_2)NbO_2$, and the latter is more stable and has very strong infrared absorptions, as listed in Table 5. The same was found for $OOTaO_2$ and $(O_2)TaO_2$. Like calculations were also done for $OOVO_2$ and $(O_2)VO_2$ using the 6-311+G* basis set, and the results are listed in Table 5.

Finally, calculations were done for the $(NbO)_2$ and $(TaO)_2$ molecules, and the rhombic structures described in Table 6 were characterized.

Discussion

The observed spectra are similar to spectra from vanadium plus oxygen experiments, and the product molecules will be assigned accordingly.

NbO. The sharp 970.6 cm^{-1} band observed after deposition is assigned to the NbO molecule based on the previous matrix work[8] and isotopic substitution. The same band was observed in Nb experiments with NO conducted in this laboratory. Annealing sharpens the 970.6 cm^{-1} band at the expense of the broader 962−965 cm^{-1} feature. A doublet structure was observed in mixed isotopic experiments. The 16/18 isotopic ratio 1.0510 is just below the harmonic diatomic ratio of 1.0511. Relative to the gas-phase value, 981.4 cm^{-1},[12] the NbO vibration

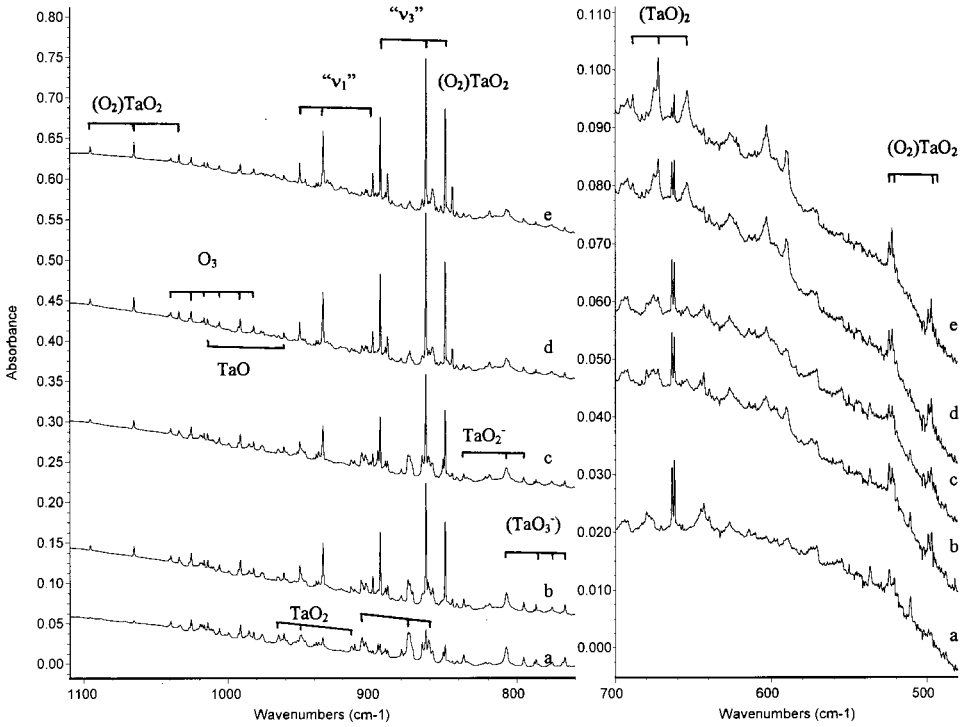

Figure 4. Infrared spectra of products formed by reactions of laser-ablated Ta atoms with O_2 (1%, scrambled $^{16}O_2 + {}^{16}O^{18}O + {}^{18}O_2$ mixture, approximately 1:2:1) in argon on condensation at 10 K: (a) co-deposited sample, (b) after 25 K annealing, (c) after broad-band photolysis for 20 m, (d) after 30 K anealing, and (e) after 35K annealing.

TABLE 3: Calculated (BP86) Geometry, Frequences (cm^{-1}), and Intensities (km/mol) for the NbO, TaO, NbO_2, and TaO_2 Molecules, Cations, and Anions

molecule	relative energy (kcal/mol)	geometry (Å, deg)	ν_1 (I)	ν_2 (I)	ν_3 (I)
$NbO(^4\Sigma)$	0	1.709	993.5(112)		
doublet	+11.0	1.704	1006.7(132)		
$NbO^+(^3E)$	+172.0	1.679	1044.2(68)		
singlet	+191.6	1.675	1057.6(71)		
TaO(doublet)	0	1.692	1036.6(68)		
quartet	+5.2	1.708	987.9(73)		
$TaO^+(^3\Sigma)$	+202.1	1.678	1040.9(51)		
singlet	+220.6	1.681	1032.6(49)		
$ONbO(^2A_1)$	0	1.738, 103.9	968.5(85)	350.7(0)	925.4(171)
$^4A_2$	+63.9	1.807, 116.5	822.0(85)	156.0(5)	297.3(11)
$ONbO^-(^1A_1)$	−37.4	1.759, 104.3	942.2(108)	336.5(0.2)	897.1(140)
triplet	−31.8	1.781, 111.4	890.5(103)	280.2(1)	853.7(193)
$ONbO^+(^1A_1)$	+185.3	1.704, 102.3	1021.0(21)	389.5(4)	981.0(133)
$OTaO(^2A_1)$	0	1.732, 104.4	977.8(36)	346.3(3)	919.9(137)
$^4A_2$	+68.8	1.795, 117.5	839.3(61)	143.9(8)	461.4(18)
$OTaO^-(^1A_1)$	−48.3	1.756, 107.4	943.4(66)	305.1(4)	885.6(160)
triplet	−28.9	1.772, 111.3	898.6(76)	268.7(3)	845.4(174)
$OTaO^+(^1A_1)$	+203.6	1.704, 102.8	1019.3(12)	379.5(3)	968.7(105)

TABLE 4: Calculated (BP86) Geometry, Vibrational Frequencies (cm^{-1}), and Intensities (km/mol) for the NbO_3 and TaO_3 Molecules and Anions

molecule	relative energy	geometry	frequency, cm^{-1} (intensity, km/mol)
$NbO_3\ ^2A_2$	0 kcal/mol	Nb−O:1.804 Å, ∠ONbO:105.5°	229.2 (22), 229.9 (1), 234.8 (1), 553.6 (0.1), 555.3 (0.1), 891.6 (8)
$NbO_3^-\ ^1A_1$	−83.0	Nb−O:1.812 Å, ∠ONbO:112.9°	170.2 (74), 280.5 (1), 280.8 (1), 836.6 (284), 838.0 (284), 866.8 (8)
$TaO_3\ ^2A_2$	0	Ta−O:1.793 Å, ∠OTaO:104.1°	238.2 (0.2), 238.9 (13), 243.5 (0.1), 637.4 (0.3), 639.2 (0.3), 905.1 (5)
$TaO_3^-\ ^1A_1$	−82.0	Ta−O:1.803 Å, ∠OTaO:109.3°	211.4 (21), 292.9 (2), 294.6 (2), 797.2 (195), 799.2 (195), 887.7 (2)

in the argon matrix red shifted about 11 cm^{-1}, which compares favorably with the 20 cm^{-1} red-shift found for VO.[24] The present DFT calculations give a 993.5 cm^{-1} fundamental for ground-state NbO, which supports this assignment.

The 1000.1 cm^{-1} band was also observed after deposition, decreased on annealing, and showed the diatomic isotopic ratio (1.0510). We tentatively assign the 1000.1 cm^{-1} band to NbO^+. DFT calculations support but cannot comfirm this assignment: NbO^+ is calculated to have a triplet ground state with a 1044.2 cm^{-1} fundamental. We expect that broad-band photolysis, which detaches electrons from anions such as O_4^- and NbO_2^- (see below), will thereby neutralize cations present in the matrix. The sharp, weak 1000.1 cm^{-1} band showed no change on broad-band photolysis. If the weak 1000.1 cm^{-1} band is due to NbO^+, then Nb^+ cations produced by laser ablation[32] and trapped in the matrix must have a higher population than NbO^+, and therefore Nb^+ probably captures most of the electrons photo-detached from O_4^- and NbO_2^-. We note that the yield of O_4^- in these experiments is small and that photodetachment from the stable NbO_2^- anion is expected to be inefficient with the

TABLE 5: Calculated (BP86) Structure, Highest Vibrational Frequencies (cm^{-1}), and Intensities (km/mol) for VO_4, NbO_4, and TaO_4 Molecules

molecule	relative energy	frequency, cm^{-1} (intensity, km/mol)
$(O_2)NbO_2$[a] $^2A_2$	0 kcal/mol	452.0 (a_1, 28), 465.6 (b_2, 7), 930.5 (b_1, 224), 954.4 (a_1, 79), 1151.2 (a_1, 42)
$OONbO_2$[b] $^2A''$	+19.9	322.3 (6), 448.6 (30), 914.5 (190), 952.5 (74), 1237.4 (84)
$(O_2)TaO_2$[c] $^2A_2$	0	430.9 (a_1, 24),480.2 (b_2, 3), 902.4 (b_1, 199), 950.9 (a_1, 48), 1113.0 (a_1, 30)
$OOTaO_2$[d] $^2A''$	+16.2	333.4 (3), 440.5 (14), 899.5 (146), 956.9 (34), 1217.9 (126)
$(O_2)VO_2$[e] $^2A_2$	0	507.4 (b_2, 10), 513.4 (a_1, 17), 1023.8 (a_1, 78), 1029.8 (b_1, 259), 1135.7 (a_1, 59)
$OOVO_2$[f] $^2A''$	+ 22.3	331.1 (14), 503.9 (21), 1005.8 (113), 1007.4 (259), 1290.9 (68)

[a] Structure: O−O: 1.343 Å, $(O_2)-NbO_2$: 2.162 Å, (O_2)Nb−O: 1.746 Å, ∠ONbO: 110.0°, the (O_2)Nb plane bisects the NbO_2 angle. [b] O−O: 1.302 Å, OO−NbO_2: 1.999 Å, OONb−O: 1.747 Å, ∠OONb: 150.0°, ∠ONbO: 106.2°. [c] O−O: 1.357 Å, $(O_2)-TaO_2$: 2.126 Å, (O_2)Ta−O_2: 1.746 Å, ∠OTaO: 111.2°, the (O_2)Ta plane bisects the TaO_2 angle. [d] O−O: 1.307 Å, OO−TaO_2: 1.964 Å, OOTa−O_2: 1.742 Å, ∠OOTa: 145.6°, ∠OTaO: 105.1°. [e] O−O: 1.330 Å, $(O_2)-VO_2$: 1.985 Å, (O_2)V−O_2: 1.603 Å, ∠OVO: 112.9°, the (O_2)V plane bisects the VO_2 angle. [f] O−O: 1.277 Å, OO−VO_2: 1.843 Å, OOV−O_2: 1.607 Å ∠OOV: 161.0°, ∠OVO: 111.7°. Recall that VO_4 calculations used a different basis set.

TABLE 6: Calculated Structure, Vibrational Frequencies (cm^{-1}), and Intensities (km/mol) for $(NbO)_2$ and $(TaO)_2$ Molecules

molecule	geometry	frequency, cm^{-1}, (intensity, km/mol)
$(NbO)_2$ (^1A_g)	Nb−O:1.991 Å, Nb−Nb:2.214 Å, ∠NbONb:67.6°	−174.3 (0), 202.8 (2), 355.4 (17), 452.1 (0), 682.9 (185), 728.8 (0)
$(TaO)_2$ (^1A_g)	Ta−O:1.985 Å, Ta−Ta:2.211 Å, ∠TaOTa:67.7°	−190.0 (0), 205.0 (3), 340.9 (23), 346.7 (0), 666.5 (168), 730.4 (0)

mercury arc; hence, the present experiments probably produce a relatively low yield of photodetached electrons for neutralizing matrix isolated cations.

TaO. Sharp bands observed at 1014.2 and 1011.7 cm^{-1} on deposition decreased on annealing. These bands produced only pure isotopic counterparts in all of the isotopic experiments; the observed 16/18 isotopic ratio (1.0550) is slightly lower than the harmonic diatomic ratio (1.0553). These bands are assigned to TaO molecules in different matrix sites. This assignment is in good agreement with the gas-phase fundamental value (1021.7 cm^{-1}), allowing for a 7.5 cm^{-1} red shift by the matrix. Weltner and McLeod assigned bands at 1028 cm^{-1} in neon and at 1020 cm^{-1} in argon to TaO, which are close to the bands observed here.[6] The 1020/966 = 1.0559 ratio is reasonable for TaO, but we suspect that spectrometer calibration would bring the previous 1020 cm^{-1} band closer to the 1014.2 cm^{-1} band observed here. BP86 calculations gave a 1036.6 cm^{-1} harmonic fundamental, which is in accord with the observations.

The 1018.1 cm^{-1} band observed after deposition decreased proportionally more than the 1014.2 cm^{-1} band on annealing, and the isotopic ratio of 1.0551 is appropriate for the diatomic molecule. DFT calculations find a triplet ground state for TaO^+ with a 1040.9 cm^{-1} fundamental, which is just 4.3 cm^{-1} higher than the calculated TaO fundamental. It is hard to determine whether the 1018.1 cm^{-1} is due to a TaO site band or to TaO^+. Again, there was no decrease in the 1018.1 cm^{-1} band on photolysis. We prefer to assign tentatively this band to TaO^+ following the NbO^+ example.

The NbO and TaO absorptions observed after deposition subsequently decreased on annealing, indicating that these molecules were formed via reaction 1; this suggests that activitation energy is required for the reactions, even though the reactions are exothermic:[12]

$$Nb + O_2 \rightarrow NbO + O \quad \Delta E = -62 \text{ kcal/mol} \qquad (1a)$$

$$Ta + O_2 \rightarrow TaO + O \quad \Delta E = -71 \text{ kcal/mol} \qquad (1b)$$

NbO_2. The sharp bands at 875.9 and 869.8 cm^{-1} were the major product absorptions after deposition, and sharp weak 933.5 and 931.1 cm^{-1} bands are associated by annealing. These bands slightly increased on inital annealing to 25 K and then decreased on further annealing. The absorptions produced triplets in the scrambled isotopic experiment with the isotopic ratios of 1.0484 and 1.0481 for lower bands and 1.0525 and 1.0528 for upper bands, respectively. The matching asymmetries in the triplet patterns of 15.7 and 30.8 cm^{-1} and of 27.7 and 12.5 cm^{-1} show interaction between the middle components of lower symmetry and associate these bands with the same molecule. The isotopic ratios for the two lower bands were slightly lower than the diatomic NbO ratio, while the ratios of upper bands were slightly higher than the diatomic ratio. These four bands are suitable for assignment to antisymmetric and symmetric vibrations of the bent NbO_2 molecule in two different matrix sites. The antisymmetric vibrational frequencies for $Nb^{16}O_2$ and $Nb^{18}O_2$ provide a basis for calculation of a 112 ± 5° upper limit to the valence angle.[19,33] In the case of MoO_2 where seven natural Mo isotopes are available, the valence angle lower limit calculated from more than 40 apex $O^nMoO/O^{n'}MoO$ isotopic frequency pairs was 119 ± 3° and the upper limit calculated from 16 terminal $^{16}O^nMo^{16}O/^{18}O^nMo^{18}O$ isotopic frequency pairs was 125 ± 1°.[34] The true angle for NbO_2 will be on the order of 4° lower than the present 112 ± 5° upper limit, and the 103.9° value calculated by DFT is reasonable.

DFT calculations support this NbO_2 assignment. The observed ν_1 and ν_3 frequencies are 0.947 and 0.966 times the calculated values. The calculated 16/18 isotopic ratios for two modes (1.0522, 1.0493) also match the experimental values.

TaO_2. The bands at 906.9 and 904.1 cm^{-1} were the major product absorptions after deposition; these bands increased and then decreased together with weaker 965.3 and 963.0 cm^{-1} bands on higher temperature annealings. Reactions with scrambled oxygen isotopic sample produced triplets, which indicated that two equivalent O atoms are involved in the vibrations. Furthermore, the matching asymmetries in the triplet structures (15.6 and 35.0 cm^{-1} and 31.8 and 14.4 cm^{-1}) associate these bands with the same molecule. The 16/18 isotopic ratios (1.0537 and 1.0559) bracketed the diatomic value as expected for the ν_3 (antisymmetric) and ν_1 (symmetric) vibrations of the bent OTaO molecule. The valence angle upper limit[19,33,34] calculated from the $Ta^{16}O_2/Ta^{18}O_2$ isotopic ratio for ν_3 is 110 ± 5°. Due to anharmonicity in the ν_3 vibrational mode, the true angle for TaO_2 will be on the order of 4° lower than the upper limit estimated here.

The 108 ± 5° angle estimate for NbO_2 and the 106 ± 5° estimate for TaO_2 are not as accurate as the 122 ± 4° prediction for MoO_2 and the 124 ± 4° estimate for WO_2, which involved both upper and lower limit measurements from oxygen and resolved metal isotopic measurements.[34]

Weltner and McLeod assigned two bands of equal intensity at 971 and 912 cm^{-1} to the TaO_2 molecule.[6] Even though these

bands are near those assigned here to TaO_2 and calibration makes the positions uncertain, there are more serious problems with the earlier assignment. First, the bands are of the same intensity and ν_1 should be weaker than ν_3. Second, the 16/18 ratios (1.0600 and 1.0568) are too high for ν_1 and ν_3 of bent TaO_2. Third, two intermediate isotopic components were reported for each band, which suggests inequivalent oxygen atoms. We believe the earlier 971 and 912 cm^{-1} absorptions were dominated by contributions from higher oxides.

The present TaO_2 assignments are comfirmed by DFT calculations, which predict a valence angle of 104.4°, and 977.8 and 919.9 cm^{-1} symmetric and antisymmetric vibrational frequencies, respectively. The calculated frequencies are 1.014 times the experimental values, and the angle is in agreement with the upper limit determined from isotopic ν_3 frequencies.

Both NbO_2 and TaO_2 molecule absorptions were observed after deposition, and only very small intermediate components were produced in the $^{16}O_2 + {}^{18}O_2$ experiments. This indicates that the dioxides are produced mainly by insertion reactions (eq 2) that are highly exothermic based on the dissociation energies.[12−14] The growth of NbO_2 and TaO_2 on annealing shows that no activation energy is required for these reactions. During condensition with excess argon on the matrix surface, the excess reaction energy was relaxed effectively, which made it possible to trap the MO_2 molecules:

$$Nb + O_2 \rightarrow NbO_2^* \xrightarrow{\text{relax}} NbO_2 \quad \Delta E = -218 \text{ kcal/mol} \tag{2a}$$

$$Ta + O_2 \rightarrow TaO_2^* \xrightarrow{\text{relax}} TaO_2 \quad \Delta E = -228 \text{ kcal/mol} \tag{2b}$$

The stretching frequencies for NbO_2 and TaO_2 are some 60−90 cm^{-1} higher than their neighboring molecules ZrO_2 and HfO_2, which have similar 115 ± 5° valence angles.[19] Of more interest is the fact that the frequencies for TaO_2 are some 30 cm^{-1} higher than those for the lighter NbO_2 molecule. This suggests an even greater lanthanide contraction and relativistic effect for Ta relative to Nb than observed for Hf relative to Zr.[19,35] The present observations and calculations for NbO_2 show that earlier frequency estimates and deductions from electron diffraction measurements[36] are not accurate.

NbO_2^+. The doublet at 937.1 and 938.4 cm^{-1} together with the weak doublet at 988.0 and 989.7 cm^{-1} observed after deposition slightly increased on annealing to 25 K and then decreased on further annealing. The isotopic 16/18 ratios of 1.0489 and 1.0490 for the lower doublet were slightly higher than the antisymmetric frequency ratio of NbO_2, and the upper doublet ratios of 1.0521 and 1.0522 were slightly lower than the NbO_2 symmetric frequency ratio. The observed triplet isotopic structure at 937.1, 906.0, and 893.4 cm^{-1} characterizes the vibration of two equivelent oxygen atoms. These bands are about 63 and 57 cm^{-1} higher than the antisymmetric and symmetric vibrations of NbO_2, which is too far to be complexes or different matrix sites. So metal dioxide cations should be considered. DFT calculations predict the NbO_2^+ singlet ground state with 981.0 and 1021.0 cm^{-1} antisymmetric and symmetric vibration frequencies, which are 56 and 52 cm^{-1} higher than the calculated NbO_2 values. The calculated cation valence angle of 102.3° is slightly lower than the calculated NbO_2 valence angle of 103.9°. From the experimental 16/18 isotopic ratio, the valence angle upper limit is 106 ± 5°, which is slightly lower than the value (112 ± 5°) determined for NbO_2.[33,34] Again, there is no measurable decrease in the bands assigned here to NbO_2^+ on photolysis, which requires that the small population of electrons photodetached be captured by more abundant Nb^+ cations.

TaO_2^+. Similar bands were observed at 937.4 and 938.8 and at 991.5 and 993.1 cm^{-1} in Ta experiments. The stronger band exhibited a mixed isotopic triplet, which comfirmed that two equivalent oxygen atoms are involved in this vibration. The upper band 16/18 isotopic ratios (1.0559) are almost the same as with TaO_2, and the lower band ratios (1.0538 and 1.0539) are slightly higher than the TaO_2 ratios. These bands can be assigned to symmetric and antisymmetric vibrations of TaO_2^+. The TaO_2^+ cation is bent slightly more than the TaO_2 molecule; the valence angle upper limit is estimated as 108 ± 5° from antisymmetric isotopic vibration frequencies.[33,34] DFT calculations gave a 1019.3 cm^{-1} symmetric and a 968.7 cm^{-1} antisymmetric frequency and a 102.8° angle, which were very close to the experimental values. There is no measurable decrease in the bands assigned to TaO_2^+ on photolysis, and this requires that more Ta^+ from laser ablation[32] be present to capture photodetached electrons.

Charged species have been observed in a number of laser-ablated metal atom studies.[19−27] Weak O_4^+ O_3^-, and O_4^- absorptions were observed in the present experiments and verify that both isolated cations and anions are formed in the laser ablation process and can be trapped in the matrix.[26,30,31] The NbO_2^+ cation has been observed in mass spectra and is the building block for niobium oxide cluster ions.[18] Additional studies of the oxidation of niobium clusters establish the binding energy of Nb^+-O_2 to be about 7.55 eV.[17]

The absorptions of NbO_2^+ and TaO_2^+ were observed after deposition, so reaction 3 must be considered where again the matrix relaxes and stabilizes the metal dioxide (cation) product. In the gas phase, the main product of niobium cation reaction with O_2 was the diatomic cation NbO^+.[17] In the present experiments, it is not possible to tell if the MO_2^+ cations are made by reaction 3 or by photoionization of MO_2 molecules from the laser plume. It is clear from other experiments of this type that metal cations are produced by laser ablation:[32]

$$Nb^+ + O_2 \rightarrow (NbO_2^+)^* \xrightarrow{\text{relax}} NbO_2^+ \tag{3a}$$

$$Ta^+ + O_2 \rightarrow (TaO_2^+)^* \xrightarrow{\text{relax}} TaO_2^+ \tag{3b}$$

Both absorptions slightly increased on 25 K annealing, as does the ozone absorption. So the most probable mechanism is reaction 4, which is exothemic. The NbO^+ reaction with O_2 to form NbO_2^+ was observed in the gas-phase reactions:[17]

$$NbO^+ + O \rightarrow NbO_2^+ \tag{4a}$$

$$TaO^+ + O \rightarrow TaO_2^+ \tag{4b}$$

$(O_2)NbO_2$. The bands at 1109.3, 945.9, 943.5, 903.6, 900.7, and 511.3 cm^{-1} increased markedly in concert on 25 K annealing. The 945.9 and 903.6 cm^{-1} bands go together while the 943.5 cm^{-1} band tracked the 900.7 cm^{-1} band. All four of these bands produced triplet isotopic structures in the scrambled isotopic experiment, indicating that two equivalent oxygen atoms are involved in the modes. The 16/18 isotopic ratios for the 945.9 and 943.5 cm^{-1} bands are 1.0530 and 1.0529, which are appropriate for symmetric stretching of the ONbO molecule, while the 903.6 and 900.7 cm^{-1} bands exhibited antisymmetric NbO_2 stretching ratios of 1.0475 and 1.0476. These bands are 12.4 and 12.4 cm^{-1} and 27.7 and 30.9 cm^{-1} higher than the analogous NbO_2 vibrations, so a *perturbed NbO_2 molecule*

should be considered. Two bands at 1109.3 and 511.3 cm^{-1} go together, although these two bands do not track either pair of bands mentioned above, but they track with the sum of 945.9 and 943.5 cm^{-1} and the 903.6 bands plus the 900.7 cm^{-1} absorption. Note that the 1109.3 cm^{-1} band center was blue shifted about 0.2 cm^{-1} after higher temperature annealing, when the 943.5 and 900.7 cm^{-1} bands become dominant. So these bands are due to a product molecule at different matrix sites, and the site effect was less pronounced for the 1109.3 and 511.3 cm^{-1} vibrational modes. The 1.0598 isotopic ratio for the 1109.3 cm^{-1} band denotes an O−O stretching vibration, and the triplet observed at 1109.3, 1078.4, and 1046.6 cm^{-1} in the $^{16}O_2 + {}^{16}O^{18}O + {}^{18}O_2$ experiment indicates that these bands are due to an O−O subunit *with equivalent O atoms in the O_2 subunit*. The sharp triplet for the O−O subunit confirms that this new $O_2 + NbO_2$ molecule has the side bonded $(O_2)NbO_2$ structure since the O_2 subunit vibration shows equivalent atomic positions. The associated 511.3 cm^{-1} band exhibited a 1.0490 isotopic ratio, which is slightly lower than the diatomic ratio and due to an $(O_2)-Nb-O_2$ vibration. In the scrambled isotopic experiment, a broadened doublet was observed, this doublet is actually an unresolved higher multiplet. The NbO_2 antisymmetric vibration was blue shifted 27.7 cm^{-1} in $(O_2)NbO_2$, similar blue shifts were also observed for $OOVO_2$[24] and $OOCrO_2$.[21] Note that the isotopic ratio for the antisymmetric vibration (1.0475) is slightly lower than the NbO_2 ratio, which gave a 118.3° valence angle upper limit, suggesting that cyclic O_2 binding to NbO_2 slightly opened the ONbO valence angle.

The 911.5, 895.5, and 892.3 cm^{-1} and 952.3, 940.2, and 938.3 cm^{-1} bands appeared on higher temperature annealing, but in more dilute experiments these bands were weak. In addition, these bands had similar isotopic ratios with the $(O_2)NbO_2$ molecule. In the O−O stretching region, a broad band at 1131 cm^{-1} tracked with these bands. The above bands are assigned to $(O_2)_xNbO_2$ complexes with $x \geq 2$.

The identification of $OOVO_2$ must be reconsidered, as on first glance there is no reason for the $(O_2)VO_2$ and $(O_2)NbO_2$ molecules to have different structures. The $OOVO_2$ identification was first suggested by Almond and Atkins[37] from photochemical studies with $V(CO)_6$ and O_2, but the apparently compelling evidence came from laser-ablated V atom reactions[24] with $^{16}O_2 + {}^{16}O^{18}O + {}^{18}O_2$, which resolved the central mixed-isotopic component of the O−O stretching multiplet into two bands split by 1.8 cm^{-1}. This is usually interpreted to indicate *inequivalent* O atoms in the vibrational mode. However, the 18−18 component is split by Fermi resonance and the 16−18 component likewise could be so split, and the straightforward interpretation of the split mixed-isotopic component to indicate inequivalent O atoms could be incorrect.

BP86 calculations done on all three MO_4 molecules (Table 5) show that the side-bonded (O_2) structure (C_{2v}) is more stable by 16−22 kcal/mol. Furthermore, the O−O complex frequencies calculated for the side-bonded structures are in excellent agreement with the observed values whereas the end-bonded structures are predicted to absorb 86−115 cm^{-1} higher. The (O_2) complex vibration predicted at 1135.7 cm^{-1} and observed at 1127.2 cm^{-1} is, of course, calculated to have a triplet scrambled isotopic spectrum, and the 1.8 cm^{-1} splitting of the central (16−18) band then must be due to Fermi resonance between the (16−18) $V^{16,18}O_2$ fundamental band observed near 1095 cm^{-1} and the overtone of the different mixed isotopic fundamentals observed near 554 cm^{-1}.

The calculation for $(O_2)VO_2$ predicts two observable $(O_2)-V-O_2$ stretching modes at 513.4 and 507.4 cm^{-1}, which have 16/18 ratios of 1.0414 and 1.0525, respectively. Recall that two bands were observed in this region at 555.6 and 506.9 cm^{-1} with 1.0416 and 1.0495 isotopic ratios, and the latter was assigned to $(O_2)VO_2$ as a minor species. It is now clear that both 555.6 *and* 508.9 cm^{-1} bands are due to the side-bonded $(O_2)VO_2$ molecule.[24] The mixed isotopic splitting patterns of these two bands are affected by interaction between these two vibrations on symmetry lowering in the mixed isotopic species. Here we identify the major VO_4 product (site a and site b in ref *24*) as the side-bonded $(O_2)VO_2$ structure with C_{2v} symmetry.

$(O_2)TaO_2$. Similar bands at 1095.7, 950.5, 946.3, 894.5, 889.4, and 524.2 cm^{-1} were observed in the Ta + O_2 reaction and are assigned to the $(O_2)TaO_2$ molecule, again with site splitting on the TaO_2 stretching modes. The 1095.7 cm^{-1} band showed an O−O stretching isotopic ratio (1.0598) and the triplet isotopic structure, indicating that two equivalent oxygen atoms are involved in this mode for the complexed O_2 subunit. (The absence of Fermi resonance between the (16−18) NbO_2 band at 1078 cm^{-1} and the overtone of the 511 cm^{-1} fundamental is clear. The lack of Fermi resonance between the (16−18) TaO_2 band at 1065 cm^{-1} and the overtone of the fundamental near 522 cm^{-1} also follows.) The 950.5 and 946.3 cm^{-1} and 894.5 and 889.4 cm^{-1} bands exhibited symmetric and antisymmetric vibration isotopic ratios of 1.0568 and 1.0530, respectively, for a TaO_2 subunit. Both 950.5 and 894.5 cm^{-1} bands produced sharp 1/2/1 triplets and confirmed that two other equivalent oxygen atoms are involved in these modes while the 946.3 and 889.4 cm^{-1} bands both gave slightly broad intermediate components, suggesting coupling between the symmetric $(O-O)TaO_2$ and $(O_2)Ta-O_2$ stretching modes. The 524.2 cm^{-1} band exhibited the diatomic isotopic ratio of 1.0549 and at least four isotopic components. It is interesting to note that the TaO_2 antisymmetric vibration in $(O_2)TaO_2$ red shifted 12.4 cm^{-1}, while $(O_2)NbO_2$ was blue shifted on O_2 complexation. Again, the cyclic O_2 ligand slightly opened the TaO_2 valence angle (estimated 9° from isotopic ratio).

Sharp related bands at 1099.5, 944.0, and 886.2 cm^{-1} appeared on higher temperature annealing. The 944.0 and 886.2 cm^{-1} bands exhibited 1.0566 and 1.0531 isotopic ratios and triplet isotopic structures, while the 1099.5 cm^{-1} band was very weak as compared with the former two bands; all of the above absorptions were weak in dilute experiments. These bands are assigned to $(O_2)_xTaO_2$ molecules with $x \geq 2$.

The $(O_2)NbO_2$ and $(O_2)TaO_2$ absorptions grow greatly on annealing, and very weak intermediate components in the $^{16}O_2 + {}^{18}O_2$ mixed isotopic experiments suggested that these molecules are produced mainly by reaction 5:

$$O_2 + NbO_2 \rightarrow (O_2)NbO_2 \quad (5a)$$

$$O_2 + TaO_2 \rightarrow (O_2)TaO_2 \quad (5b)$$

M_2O_2 Species. The analogous vanadium experiments produced weak 1042.4 cm^{-1} and 668.1 and 504.3 cm^{-1} bands on annealing, which were suggested to be due to open VOVO and puckered ring V_2O_2 molecules.[24] An analogous band observed here for Nb at 997.6 cm^{-1}, which gave a quartet scrambled isotopic spectrum and an appropriate 16/18 isotopic ratio for an open NbONbO molecule. Weak bands near 970 cm^{-1} for Ta can only be identified as Ta_xO_y. The 689.1 and 622.4 cm^{-1} absorptions that appear on annealing for Ta could be due to $(TaO)_2$ species; both bands exhibit triplet scrambled isotopic patterns and diatomic 16/18 isotopic ratios. The 689.1 cm^{-1} band is appropriate for a bridged Ta−O vibration, and the 689.1 cm^{-1} band is assigned to the rhombus $(TaO)_2$ molecule.

Analogous rhombic transition metal oxides have been characterized for the later first-row transition metal atoms Mn−Ni.[20,22,25,38]

The $(TaO)_2$ molecules are formed by reaction 6, according to triplet structures observed in both mechanical and scrambled isotopic mixture experiments: The weak band at 687.6 cm^{-1}

$$TaO + TaO \rightarrow (TaO)_2 \quad (6)$$

in the niobium system also increased on annealing but showed a lower 16/18 ratio near that for ONbO and no obvious intermediate component. This band cannot be identified.

MO_2^-. The sharp 854.1 cm^{-1} band with Nb increased slightly on 25 K annealing, decreased slightly on broad-band photolysis, and decreased steadily on subsequent annealings. The band revealed an asymmetric triplet on statistical oxygen isotopic substitution, which is appropriate for the vibration of two equivalent oxygen atoms interacting with a higher frequency mode. DFT calculations predict the strong NbO_2^- anion fundamental some 28 cm^{-1} below the neutral NbO_2 molecule, and the 854.1 cm^{-1} band is an appropriate assignment. The 836.9 cm^{-1} band with Ta can, for the same evidence and reasons, be assigned to TaO_2^-. The 16/18 ratios predict 131° angle upper limits[33,34] for both anions, somewhat larger than the 104° and 107° DFT values, but neither method is expected to be highly accurate. Nevertheless, the valence angles for NbO_2^- and TaO_2^- are clearly larger than valence angles for NbO_2 and TaO_2, and near values recently determined for the isoelectronic molecules MoO_2 and WO_2 (122 ± 4° and 124 ± 4° valence angle upper limit−lower limit averages).[34] In this regard, both Cr and O isotopic frequencies for CrO_2 have accurately determined the valence angle as 128 ± 4°.[21] The analogous relationships have been found for ZrO_2 and ZrO_2^- and for HfO_2 and HfO_2^-.[19]

The NbO_2^- and TaO_2^- anions are made by the capture of electrons from the laser ablation process[32] during sample condensation:

$$NbO_2 + e^- \rightarrow NbO_2^- \quad (7a)$$

$$TaO_2 + e^- \rightarrow TaO_2^- \quad (7b)$$

The slight decrease in NbO_2^- and TaO_2^- absorptions on photolysis is due either to photodissociation (eq 8a) or photodetachment (eq 8b):

$$NbO_2^- \rightarrow NbO^- + O \quad (8a)$$

$$NbO_2^- \rightarrow NbO_2 + e^- \quad (8a)$$

It is expected that NbO_2 should have an appreciable electron affinity[39] such that photodetachment with the mercury arc will be an inefficient process.

MO_3^-. The 817.1 cm^{-1} band observed with Nb after deposition increased slightly on 25K annealing and decreased on photolysis and higher temperature annealing. This band shifted to 781.4 cm^{-1} with $^{18}O_2$ and gave the 16/18 isotopic ratio of 1.0457, which is lower than the diatomic ratio and indicative of an antisymmetric O−Nb−O vibration. In both mixed and scrambled isotopic experiments, a quartet with mixed isotopic counterparts at 794.3 and 787.1 cm^{-1} was observed, which suggested three equivalent oxygen atoms involved in a degenerate mode.[40] Accordingly, the 817.1 cm^{-1} band is assigned to a NbO_3 species.

The 807.0 cm^{-1} band in the Ta + O_2 system has the same behavior: observed after deposition, slightly increased on 25 K annealing, decreased on photolysis, and then decreased on higher annealing cycles. The 16/18 isotopic ratio of 1.0523 is lower than the diatomic Ta−O ratio. The quartet observed in both mechanical and scrambled isotopic experiments points to a degenerate mode, which suggests a trigonal TaO_3 species.

The DFT calculations suggest the anion identification. The NbO_3^- anion is predicted to have a very strong ν_3(e) fundamental near 837 cm^{-1}, to have a valence angle near 113°, and to be 83.0 kcal/mol more stable than NbO_3 with a weak ν_3(e) mode at 892 cm^{-1} and a 105° valence angle. Although we have observed no absorptions that can be assigned to NbO_3, the 817.1 cm^{-1} band is more likely due to NbO_3^-. Likewise, the TaO_3^- anion is predicted to have a strong ν_3 fundamental near 700 cm^{-1} and to be 82.0 kcal/mol more stable than TaO_3. The CCl_4 doping experiments described below confirm that these absorptions are due to anions.

The MO_3 molecules can be made by reactions 9, and the corresponding anions can be made by reactions 10. The NbO_3 molecule was found to be the building block for large niobium oxide clusters:[18]

$$MO_2 + O \rightarrow MO_3 \quad (9a)$$

$$MO + O_2 \rightarrow MO_3 \quad (9b)$$

$$MO_2 + O^- \rightarrow MO_3^- \quad (10a)$$

$$MO_3 + e^- \rightarrow MO_3^- \quad (10b)$$

We are investigating the effect of doping the matrix sample with CCl_4 (0.05%) on the population of product species trapped in the matrix. Carbon tetrachloride is an efficient electron trap, and in other studies in this laboratory, we have shown that CCl_4 doping *reduces* anion absorbances by 90−100% and *increases* cation relative to neutral molecule absorbances by 50−100%. In O_2 experiments, CCl_4 doping eliminates O_4^- while O_4^+ is clearly observed. In the present O_2 reactions with laser-ablated Nb and Ta, CCl_4 doping has the same effect and supports the present product identifications. The bands assigned here to NbO_2^-, NbO_3^-, TaO_2^-, and TaO_3^- are eliminated with CCl_4 added, whereas the ν_1 and ν_3 NbO_2^+ and TaO_2^+ absorptions are increased to the intensities observed for NbO_2 and TaO_2. The NbO^+ and TaO^+ absorptions are weaker and masked by CCl_4 and photolysis product absorptions so that additional supporting evidence cannot be obtained.

A similar experiment with V and O_2, doped CCl_4, and low laser energy (4 ± 1 mJ/pulse) eliminated the 896.8, 894.8 cm^{-1} bands assigned earlier[24] to ν_3 of VO_2^-. Weak unassigned bands in the V + O_2 system at 886.5, 883.9 cm^{-1} (844.7, 842.1 cm^{-1} for $^{18}O_2$) and 916.2 cm^{-1} (883.3 cm^{-1} for $^{18}O_2$) are assigned here to ν_1 of VO_2^- and ν_3 of VO_3^-, respectively; these latter bands were also eliminated by CCl_4 doping. A similar DFT calculation for VO_3^- predicts a D_{3h} structure with one very strong band, ν_3, at 977.1 cm^{-1} and the low 16/18 ratio 1.03693, both in excellent agreement with observed values. Unfortunately, no absorptions can be assigned to cations in the V + O_2 system.

Other Absorptions. The weak doublet at 861.3 and 859.4 cm^{-1} in the Nb + O_2 system and weak bands in the N−N stretching region at 2107.0 cm^{-1} go together and are assigned to $(N_2)NbO_2$ as will be discussed in another paper. Several

weak absorptions cannot be identified from the present observations and are noted by Nb_xO_y and Ta_xO_y in Tables 1 and 2.

Conclusions

Laser-ablated niobium and tantalum atoms react with O_2 to give MO and OMO as major products and MO^+, MO_2^-, and MO_2^+ as minor products, which are identified from oxygen isotopic substitution on their matrix infrared spectra and from DFT calculations of isotopic frequencies. Annealing allows diffusion and further reactions to give $(O_2)MO_2$ complexes with C_{2v} structures. Similar calculations and a re-analysis of the V + O_2 observations show that the analogous vanadium species is also $(O_2)VO_2$.

On the basis of the ν_3 vibrational frequencies for the $M^{16}O_2$ and $M^{18}O_2$ molecules, the metal dioxide valence angles are estimated to be 108 ± 5° for NbO_2 and 106 ± 5° for TaO_2; the molecular cations are more bent with valence angles 103 + 5° and 105 ± 5° for NbO_2^+ and TaO_2^+, respectively; and the NbO_2^- and TaO_2^- molecular anions are more open with 120 ± 10° valence angles allowing for anharmonicity.[33] Evidence is also presented for stable MO_3^- anions. The CCl_4 doping investigations confirm these identifications of charged species. Charged species, formed by laser-plume photoionization or capture of electrons produced in the ablation process, make a minor contribution to the observed spectrum. Laser ablation of metal atoms for reaction with O_2 is an effective method of preparing small refractory oxides, and it offers the advantage of minimum heat load on the matrix in contrast to conventional high-temperature oven techniques.

Acknowledgment. We gratefully acknowledge NSF support for this work under Grant CHE 97-00116.

References and Notes

(1) Wachs, I. E. *Proc. Int. Conf. Niobium Tantalum* **1989**, 679.
(2) Rao, V. R. *Indian J. Phys*. **1950**, *24*, 35.
(3) Premaswarup, D. *Nature* **1955**, *175*, 1003.
(4) Premaswarup, D.; Barrow, R. F. *Nature* **1957**, *180*, 602.
(5) Rao, V. R.; Premaswarup, D. *Indian J. Phys*. **1953**, *27*, 399.
(6) Weltner, W., Jr.; McLeod, D., Jr. *J. Chem. Phys*. **1965**, *42*, 882.
(7) Cheetham, C. J.; Barrow, R. F. *Trans. Faraday Soc*. **1967**, *63*, 1835.
(8) Green, D. W.; Korfmacher, W.; Gruen, D. M. *J. Chem. Phys*. **1973**, *58*, 404.
(9) Brom, J. M., Jr.; Durham, C. H., Jr.; Weltner, W., Jr. *J. Chem. Phys*. **1974**, *61*, 970.
(10) Brittain, R.; Powell, D.; Kreglewski, M.; Vala, M. *Chem. Phys*. **1980**, *54*, 71.
(11) Vala, M.; Brittain, R. D.; Powell, D. *Chem. Phys*. **1985**, *93*, 147.
(12) Huber, K. P.; Herzberg, G. *Molecular Spectra and Molecular Structure*; Van Nostrand: New York, 1979.
(13) Inghram, M. G.; Chupka, W. A.; Berkowitz, J. *J. Chem. Phys*. **1957**, *27*, 569.
(14) Balducci, G.; Gigli, G.; Guido, M. *J. Chem. Phys*. **1986**, *85*, 5955.
(15) Dyke, J. M.; Ellis, A. M.; Feher, M.; Morris, A.; Paul, A. J.; Stevens, J. C. H. *J. Chem. Soc., Faraday Trans. 2* **1987**, *83*, 1555.
(16) Loh, S. K.; Lian, L.; Armentrout, P. B. *J. Chem. Phys*. **1989**, *91*, 6148.
(17) Radi, P. P.; Helden, G. W.; Hsu, M. T.; Kemper, P. R.; Browers, M. T. *Int. J. Mass Spectrom. Ion Processes* **1991**, *109*, 49.
(18) Deng, H. T.; Kerns, K. P.; Castleman, A. W., Jr. *J. Phys. Chem*. **1996**, *100*, 13386.
(19) Chertihin, G. V.; Andrews, L. *J. Phys. Chem.* **1995**, *99*, 6356.
(20) Chertihin, G. V.; Saffel, W.; Yustein, J. T.; Andrews, L.; Neurock, M.; Ricca, A.; Bauschlicher, C. W., Jr. *J. Phys. Chem*. **1996**, *100*, 5261.
(21) Chertihin, G. V.; Bare, W. D.; Andrews, L. *J. Chem. Phys*. **1997**, *107*, 2798.
(22) Citra, A.; Chertihin, G. V.; Andrews, L.; Neurock, M. *J. Phys. Chem. A* **1997**, *101*, 3109.
(23) Chertihin, G. V.; Andrews, L.; Bauschlicher, C. W., Jr. *J. Phys. Chem. A* **1997**, *101*, 4026.
(24) Chertihin, G. V.; Bare, W. D.; Andrews, L. *J. Phys. Chem. A* **1997**, *101*, 5090.
(25) Chertihin, G. V.; Andrews, L. *J. Phys. Chem. A* **1997**, *101*, 8417.
(26) Chertihin, G. V.; Andrews, L. *J. Chem. Phys.* **1998**, *108*, 6404.
(27) Burkholder, T. R.; Andrews, L. *J. Chem. Phys*. **1991**, *95*, 8697.
(28) Andrews, L.; Burkholder, T. R.; Yustein, J. T. *J. Phys. Chem*. **1992**, *96*, 10182.
(29) (a) Andrews, L.; Spiker, R. C., Jr. *J. Phys. Chem.* **1972**, *76*, 3208. (b) Spiker, R. C., Jr.; Andrews, L. *J. Chem. Phys.* **1973**, *59*, 1851. (c) Andrews, L.; Ault, B. S.; Grzybowski, J. M.; Allen, R. O. *J. Chem. Phys.* **1975**, *62*, 2461.
(30) (a) Andrews, L. *J. Chem. Phys.* **1971**, *54*, 4935. (b) Thompson, W. E.; Jacox, M. E. *J. Chem. Phys.* **1989**, *91*, 3826. (c) Hacaloglu, J.; Andrews, L. To be published. The weak 1118 cm^{-1} band is due to O_4^+.
(31) Frisch, M. J.; Trucks, G. W.; Schlegel, H. B.; Gill, P. M. W.; Johnson, B. G.; Robb, M. A.; Cheeseman, J. R.; Keith, T.; Petersson, G. A.; Montgomery, J. A.; Raghavachari, K.; Al-Laham, M. A.; Zakrzewski, V. G.; Ortiz, J. V.; Foresman, J. B.; Cioslowski, J.; Stefanov, B. B.; Nanayakkara, A.; Challacombe, M.; Peng, C. Y.; Ayala, P. Y.; Chen, W.; Wong, M. W.; Andres, J. L.; Replogle, E. S.; Gomperts, R.; Martin, R. L.; Fox, D. J.; Binkley, J. S.; Defrees, D. J.; Baker, J.; Stewart, J. P.; Head-Gordon, M.; Gonzalez, C.; Pople J. A. *Gaussian 94, Revision B.1*; Gaussian, Inc.: Pittsburgh, PA, 1995.
(32) (a) Kang, H.; Beauchamp, J. L. *J. Phys. Chem.* **1985**, *89*, 3364. (b) Zhou, M.-F.; Fu, Z.; Qin, Q. *Appl. Surf. Sci.* **1998**, *125*, 208.
(33) Allavena, M.; Rysnik, R.; White, D.; Calder, V.; Mann, D. E. *J. Chem. Phys.* **1969**, *50*, 3399.
(34) Bare, W. D.; Souter, P. F.; Andrews, L. *J. Phys. Chem. A*, in press. (MoO_2, WO_2).
(35) Pyykko, P. *Chem. Rev.* **1988**, *88*, 563.
(36) Gershikov, A. G.; Spiridonov, V. P.; Prikhod'ko, A. Ya.; Erokhin, E. V. *High Temp. Sci.* **1981**, *14*, 17.
(37) Almond, M. J.; Atkins, R. W. *J. Chem. Soc., Dalton Trans.* **1994**, 835.
(38) Chertihin, G. V.; Citra, A.; Andrews, L.; Bauschlicher, C. W., Jr. *J. Phys. Chem. A* **1997**, *101*, 8793.
(39) The electron affinity of FeO_2 is 2.36 eV: see Fan, J.; Wang, L.-S. *J. Chem. Phys.* **1995**, *102*, 8714. The electron affinity of CuO_2 is 3.46 eV: see (a) Wu, H.; Desai, S. R.; Wang, L.-S. *J. Chem. Phys.* **1995**, *103*, 4363. (b) Wu, H.; Desai, S. R.; Wang, L.-S. *J. Phys. Chem. A* **1997**, *101*, 2103.
(40) Darling, J. H.; Ogden, J. S. *J. Chem. Soc., Dalton Trans.* **1972**, 2496.